Vulnerability of industrial plants to flood-induced natechs: A Bayesian network approach

Khakzad, N.; van Gelder, Pieter

DOI
10.1016/j.ress.2017.09.016

Publication date
2017

Document Version
Accepted author manuscript

Published in
Reliability Engineering & System Safety

Citation (APA)
Khakzad, N., & van Gelder, P. (2017). Vulnerability of industrial plants to flood-induced natechs: A Bayesian network approach. *Reliability Engineering & System Safety*. https://doi.org/10.1016/j.ress.2017.09.016

Vulnerability of industrial plants to flood natechs: A Bayesian network approach

Nima Khakzad , Pieter Van Gelder

PII: S0951-8320(17)30504-5
DOI: 10.1016/j.ress.2017.09.016
Reference: RESS 5954

To appear in: *Reliability Engineering and System Safety*

Received date: 26 April 2017
Revised date: 1 September 2017
Accepted date: 28 September 2017

Please cite this article as: Nima Khakzad , Pieter Van Gelder , Vulnerability of industrial plants to flood natechs: A Bayesian network approach, *Reliability Engineering and System Safety* (2017), doi: 10.1016/j.ress.2017.09.016

Highlights

- A methodology has been developed for natech risk assessment of industrial plants.
- Flotation, shell buckling, and rigid sliding are considered as prevailing failure modes.
- Physical reliability models and Monte Carlo simulation are used to generate artificial failure data.
- Bayesian parameter learning is used to estimate and combine failure probabilities.

Vulnerability of industrial plants to flood natechs: A Bayesian network approach

Nima Khakzad*, Pieter Van Gelder

Safety and Security Science Group, Delft University of Technology, The Netherlands

*Corresponding author: n.khakzadrostami@tudelft.nl, Phone: +31 15 2784709
Address: Jaffalaan 5, Building 31, Delft 2628 BX, The Netherlands

Abstract

In the context of natural-technological (natech) accidents, flood-induced damage of industrial plants have received relatively less attention mainly due to the scarcity of such accidents compared to those triggered by earthquakes, high winds, and lightnings. The large amount of oil spillage due to floods triggered by the Hurricanes Katrina and Rita in 2005 in the U.S. demonstrated the potential of floods in causing catastrophic natechs. In the present study, we have developed a methodology based on physical reliability models and Bayesian network so as to assess the fragility (probability of failure) of industrial plants to floods. The application of the methodology has been demonstrated for petroleum storage tanks where flotation, shell buckling, and sliding are considered as the prevailing failure modes. Due to scarcity of empirical data and high-resolution field observations prevailing in natechs, the developed methodology can effectively be applied to a wide variety of natechs in industrial plants as long as limit state equations of respective failure modes can reasonably be developed.

Keywords: Floods; Natech accidents; Petroleum storage tank; Physical reliability models; Bayesian network.

1. Introduction

Technological accidents which are triggered by natural events such as earthquake, lightning, storm, wildfire, tsunami, and flood are known as natech (natural-technological) accidents. Natural disasters have reportedly led to the release of significant amounts of oil, chemicals, and radiological substances (Showalter and Myre, 1994; Rasmussen, 1995; Young et al., 2004).

The occurrence of natechs in industrial plants, particularly chemical facilities, can result in catastrophic consequences in terms of large spillage of hazardous materials which with the assistance of flood discharge can vastly spread and cause enormous environmental damages (Figure 1). In 2005, the floods triggered by the Hurricanes Katrina and Rita in the U.S. caused a spillage of about 8 million gallons of oil into the ground and waterways from Louisiana to Alabama, the second largest oil spill disaster in the U.S. after the 2010 BP spill in the Gulf of Mexico (Sturgis, 2015). In August 2017, the Hurricane Harvey in the U.S. caused damage to storage tanks in refineries and petrochemical plants, leading to substantial release of pollutants[1]. Aside from direct structural damage to industrial plants, the power outage in a chemical facility coupled with damaged backup generators made an extremely flammable chemical (organic peroxides) – which must be kept refrigerated – degrade and catch fire (the guardian, 2017). The structural damage caused by natural events at industrial plants, however, does not compare with the environmental damage and revenue losses due to interruption in production and supply chain: the Hurricane Harvey made oil refineries shut down their operations in the wake of heavy rainfall and flooding, leading to at least a loss of more than 1 million barrels per day in refining capacity (CNBC, 2017).

Figure 1. An aerial image of the oil spill that contaminated residential neighborhoods in Louisiana's St. Bernard Parish after Hurricane Katrina. (source: Environmental Protection Agency, the U.S.)

Risk of natech accidents has started to be recognized in quantitative risk assessment of industrial plants since the last decade (Young et al., 2004; Cruz and Okada, 2008; Antonioni et al, 2009; Krausmann et al., 2011). Most of the attempts in the field of natech risk assessment have been devoted to the fragility assessment of industrial plants to earthquakes (Salzano et al., 2003, 2009; Campedel et al., 2008; Korkmaz et al., 2011; Girgin and Krausmann, 2013; Marzo et al., 2015), lightning (Renni et al., 2010; Necci et al., 2013, 2016), tsunami (Cruz et al., 2011; Mebarki et al., 2016; Basco and Salzano, 2016) and volcanic ashes (Millazzo et al., 2013). Despite an extensive literature in flood assessment and flood-induced damage of structures and infrastructures (Vrijling, 2001; Buijs et al., 2009; Jonkman et al., 2010; Hong et al., 2015; Sattele et al., 2015), relevant work in the context of flood natechs (impact of floods on industrial plants) has been very few (Haptmanns, 2010; Landucci et al., 2012, 2014; Antonioni et al., 2015; Khakzad and Van Gelder, 2017). This has partly been due to the rarity of flood natechs (Cozzani et al., 2010) and partly due to the scarcity of high resolution historical or experimental data relating the characteristics of floods (return period, inundation height, flow speed) to the damage states of impacted vessels (Godoy, 2007; Campedel,

[1]At the time of submitting the present study, the Hurricane Harvey was still hitting the Houston area in the U.S., and thus the accurate extent of damage to industrial plants had not yet been known.

2008; Krausmann and Mushtaq, 2008; Santella et al., 2010). For example, in most of accident reports and previous studies, it is not clarified if the spillage of chemicals during floods has been due to disconnected pipelines or due to the structural collapse of vessels (Cozzani et al., 2010).

Investigating 272 flood natech accidents from 1960 to 2007 in Europe and the U.S., Cozzani et al. (2010) identified the above-ground storage tanks as the most frequently damaged equipment (74% of cases), including atmospheric storage tanks, floating roof tanks, and pressurized tanks. Besides, the displacement of equipment (due to flotation or sliding), shell buckling, and impact with debris have been identified as credible failure modes (Cozzani et al., 2010). Similar failure modes have been reported in Godoy (2007) based on the site observations of affected process plants in Louisiana and Texas, U.S., after Hurricane Katrina in 2005. It is also worth mentioning that the pipeline disconnection as a lateral failure mode resulting from the displacement of equipment has reportedly led to significant chemical releases as well (Godoy, 2007; Campedel, 2008; Cozzani et al., 2010).

Due to the scarcity of historical data, the majority of previous quantitative risk assessment studies has relied on analytical or numerical techniques to calculate the probability of failure based on the failure mechanism of impacted vessels subject to floods (Landucci et al., 2012, 2014; Kameshwar and Padgett, 2015; Mebarki et al., 2016; Khakzad and Van Gelder, 2017). In this regard, usually based on a comparison between the flood loads and the vessel resistance, limit state equations (LSEs) have been developed for different failure modes of the vessel which in turn can be used to determine the likelihood of failures deterministically (Landucci et al., 2012, 2014) or probabilistically (Kameshwar and Padgett, 2015; Mebarki et al., 2016).

Regardless of the followed approach, in the previous studies usually merely one failure mode has been investigated (e.g., Landucci et al., 2012, 2014) and where more than one failure mode have been considered (Kameshwar and Padgett, 2015) the resulting failure probabilities have been aggregated assuming independent failure modes. This latter oversimplification, however, may result in an overestimation of the total failure probability since the same parameters (load-resistance forces) contribute to the failure modes of an impacted vessel, making them conditionally dependent. To address this drawback, Khakzad and van Gelder (2017) developed a methodology based on Bayesian network (BN) to facilitate the incorporation of dependencies among individual failure modes.

The present study is aimed at presenting a methodology based on physical reliability modes and BN to assess the vulnerability of above-ground atmospheric storage tanks (hereafter, storage tanks) to floods. The main idea, in a nutshell, is first to generate artificial failure data based on failure mechanism of storage tanks (a failure takes place if the random stress on the storage tank exceeds the random strength of the storage tank) and Monte Carlo simulation, and then to apply Bayesian parameter learning to estimate and combine failure probabilities. The methodology is schematically displayed in Figure 2, comprising the following four parts:

(i) physics of failure analysis (Steps 1-3), where the loading and resisting forces contributing to the failure of storage tanks during floods are investigated. Based on such, LSEs will be developed for respective failure modes.

(ii) data generation (Steps 4-6), where Monte Carlo simulation is used to generate random values of LSEs based on the random variables involved in loading-resisting parameters.

(iii) development of BN (Steps 7 and 8), where the structure of the BN, i.e., the nodes and their conditional dependencies in form of arcs, is constructed. Moreover, using the BN structure and the data generated in the previous part the parameters of the BN (i.e., conditional probabilities) are estimated using maximum likelihood (or log-likelihood) estimation technique. Having the structure G and the parameters θ of the BN (G, θ), it can be used for predicting the failure probabilities.

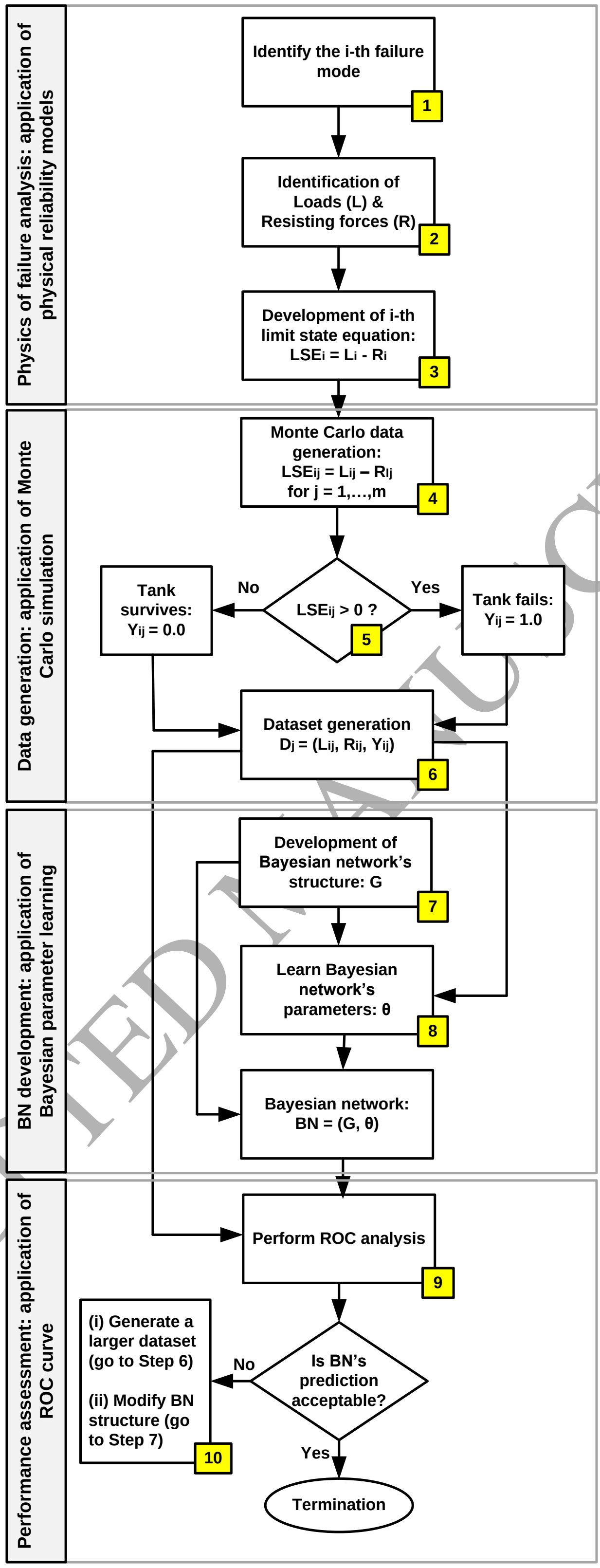

Figure 2. Schematic of the developed methodology.

(iv) performance assessment (Steps 9 and 10), where by making a comparison between the failure probabilities predicted by the BN (Part iii) and the data generated based on LSEs (Part ii), the performance of the BN as a classifier (whether the storage tank fails or not) can be assessed using the technique of Receiver Operating Characteristics (ROC). If the BN turns out to be performing poorly, its performance should be improved either by using a larger dataset (if the poor performance is attributed to, among others, incomplete observation data) or by modifying the structure of the BN which would otherwise fail to capture the dependencies among the contributing factors.

The remaining of the paper has been organized as follow: in Section 2, the physics of failure (failure modes) of storage tanks impacted by floods will be modeled using simplified LSEs. These equations will later be coupled with Monte Carlo simulation to generate data required for BN development. In Section 3, the basics of BN, Bayesian parameter learning, and ROC are presented. The application of the methodology will be exemplified in Section 4, while the conclusions are presented in Section 5.

2. Flood-induced failure modes

2.1. Flotation

Flotation of storage tanks has reportedly been the most prominent failure mode observed due to the floods triggered by Hurricane Katrina (Godoy, 2007; Santella et al., 2010). To investigate the physical conditions leading to the flotation of a storage tank during flood, (i) the weight of the tank bulk W_T, (ii) the weight of the contained chemical W_L, and (iii) the force exerted by the foundation F_F are considered as resisting forces; on the other hand, the buoyant force F_B of flood (White, 2003) is considered as the loading force as depicted in Figure 3. In the figure, *D*, *H*, and *t* are the tank's diameter, height, and shell thickness, respectively, while the height of the chemical inside the tank and the flood inundation depth have been denoted, respectively, by *h* and *S*. Although the specifications for the anchorage of storage tanks have been given in the current standards (e.g., API, 650), the common design practice in many chemical plants is still based on self-anchored storage tanks, i.e., $F_F = 0$ (Godoy, 2007).

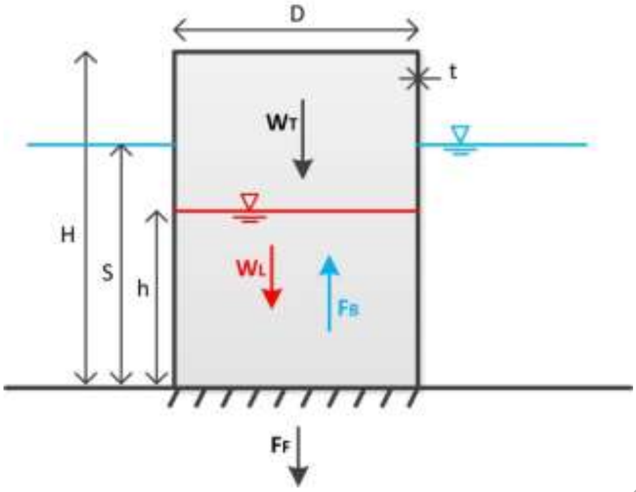

Figure 3. Schematic of the load-resistance forces considered in tank flotation.

Considering the forces in Figure 3, the flotation limit state equation, $LSE_{Flotation}$, can be developed in Equations (1)-(5):

$$LSE_{Floatation} = F_B - W_T - W_L \tag{1}$$

$$F_B = \rho_w g \frac{\pi D^2}{4} S \tag{2}$$

$$W_T = \rho_s g \left(\pi D H + 2\frac{\pi D^2}{4}\right) t \tag{3}$$

$$W_L = \rho_l g \frac{\pi D^2}{4} h \tag{4}$$

where ρ_w, ρ_s, and ρ_l are the densities of the flood water, tank shell (usually steel), and the chemical substance inside the tank, respectively; g is the gravitational acceleration. As can be seen from Equation (1), the storage tank will float if $LSE_{Flotation} > 0$.

2.2. Shell buckling

As reported by Godoy (2007), the shell buckling of storage tanks was mainly caused by high winds during the Hurricanes Katrina and Rita rather than by the subsequent floods. However, Campedel (2008), Cozzani et al. (2010), and Landucci et al. (2012) have pointed out the shell buckling as a potential failure mode, where an external pressure above the critical pressure P_{cr} may lead to the shell collapse.

To investigate the physical conditions leading to the shell buckling, the main internal (resisting) and external (loading) radial pressures on the shell have been depicted in Figure 4. The radial pressures include the hydrostatic pressure both from the height of liquid inside the tank P_L (resisting) and from the height of flood inundation P_s (loading) and the hydrodynamic pressure P_d (loading) due to the kinetic energy of the flood flow (White, 2003). If the resultant of the radial pressures are higher than a critical pressure P_{cr}, shell buckling occurs. As a result, the corresponding LSE can be developed in Equation (5).

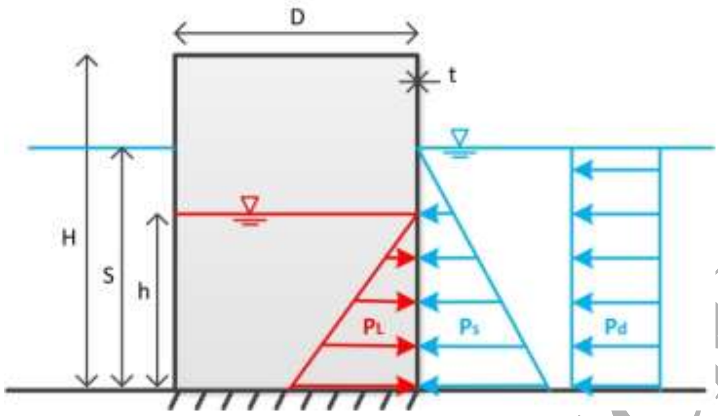

Figure 4. Schematic of the load-resistance forces considered for shell buckling.

$$LSE_{Buckling} = P_s + P_d - P_L - P_{cr} \tag{5}$$

$$P_L = \rho_l g h \tag{6}$$

$$P_s = \rho_w g S \tag{7}$$

$$P_d = \frac{1}{2} C_d \rho_w V^2 \tag{8}$$

where C_d is the drag coefficient (C_d = 2.0 for square and rectangular piles, and C_d = 1.2 for round piles); V is the average speed of the flow. For cylindrical shell structures, the amount of buckling critical pressure P_{cr} can be calculated using simplified relationships given in Equations (9) and (10) for long cylinders (Iturgaiz Elso, 2012) and short cylinders (Landucci et al., 2012), respectively. Above-ground storage tanks usually lie in the category of short cylinders.

$$P_{cr} = \frac{E}{1-v^2}\left(\frac{t}{D}\right)^3 \tag{9}$$

$$P_{cr} = \frac{2Et}{D}\left\{\frac{1}{(n^2-1)\left[1+\left(\frac{2nH}{\pi D}\right)^2\right]^2} + \frac{t^2}{3(1-v^2)D^2}\left[n^2 - 1 + \frac{2n^2-1-v}{\left(\frac{2nH}{\pi D}\right)^2 - 1}\right]\right\} \quad \text{for} \quad n \geq 2 \tag{10}$$

where E is the Young's modulus of the tank material; v is Poisson ratio; n is the number of waves involved in buckling. As can be seen from Equation (5), the tank shell will buckle if $LSE_{Buckling} > 0$.

2.3. Sliding

As for unanchored storage tanks, the rigid sliding due to the hydrodynamic pressure of the flood surge has been reported as a possible failure mode (Cozzani et al., 2010) but not so common as flotation and shell buckling. Considering the storage tank and its containment as a body of mass, the hydrodynamic force of the flood (load) and the friction force between the tank and the ground (resistance) are taken into account as influential forces (Figure 5). The limit state equation can be presented in Equation (11).

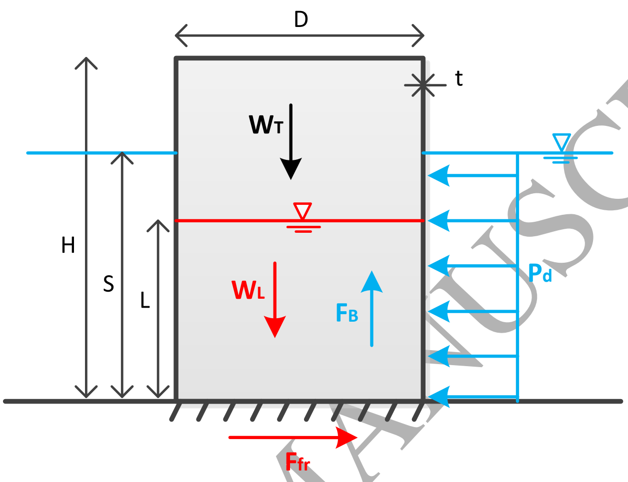

Figure 5. Schematic of the load-resistance forces considered for sliding.

Accordingly, the hydrodynamic force F_d can be calculated as the product of the hydrodynamic pressure P_d and the vertical wet section area of the storage tank in Equation (12). The friction force F_{fr} is equal to the product of the friction coefficient C_f and the normal force F_N exerted from the ground to the bottom of the tank, as presented in Equation (13). For an unanchored storage tank, the normal force is the vector summation of the weight of the tank, weight of chemical, and the buoyant force, as shown in Equation (14), as long as the tank is not floated. Having the load, F_d, and the resistance, F_{fr}, the corresponding LSE has been developed in Equation (11), where $LSE_{Sliding} > 0$ implies the tank's sliding.

$$LSE_{Sliding} = F_d - F_{fr} \tag{11}$$

$$F_d = P_d DS \tag{12}$$

$$F_{fr} = C_f F_N \tag{13}$$

$$F_N = W_T + W_L - F_B \tag{14}$$

where C_f is the friction coefficient (0.4 according to API 650). It should be noted that the existence of the friction force is legitimate as long as the tank stays in touch with the ground; in other words, if the flotation occurs first, the sliding will be excluded from the analysis. Such conditional dependency between flotation and sliding should be taken into account in BN modeling.

3. Bayesian network modelling

3.1. Bayesian network

BN (Pearl, 1988) is a directed acyclic graph that represents a joint probability distribution of a set of random variables U= {X_1, X_2, …, X_n}. The network can be defined as BN= (G, θ); G is the structure of the graph where the random variables are presented as nodes and direct dependencies among the random variables are denoted as arcs between the nodes. The graph G satisfies Markovian condition in that each variable in G is independent of its nondescendents given its immediate parents. As a result, the associated joint probability distribution of the random variables can be factorized as the multiplication of conditional probabilities of each node (variable) given its parent nodes as:

$$P(X_1, X_2, \dots, X_n) = \prod_{i=1}^{n} P(X_i | pa(X_i)) \tag{15}$$

The conditional probabilities of type $\theta_i = P(X_i|pa(X_i)$ are also known as the network parameters which can either be elicited from subject matter experts – usually in case of small networks – or be learned from data.

3.2. Bayesian parameter learning

Suppose we have a dataset comprising m complete observations of the random variables as $D = \{(X_1^j, X_2^j, \dots, X_n^j), j = 1, \dots, m\}$ in that each observation assigns a value to each variable. Accordingly, the log-likelihood function of the network parameters can be developed as:

$$Log - Like(D; G, \theta) = log(P(D|\theta) = \sum_{j=1}^{m} log\, P(X_1^j, X_2^j, \dots, X_n^j|\theta) = \sum_{j=1}^{m} log \prod_{i=1}^{n} P\left(X_i^j \middle| pa(X_i^j)\right) = \sum_{j=1}^{m} \sum_{i=1}^{n} log\, \theta_i^j \tag{16}$$

Maximizing the log-likelihood function given in Equation (16) with respect to θ, the parameters of the BN can be estimated. Applications of Bayesian parameter learning in probabilistic risk assessment can be found in Siu and Kelly (1998), Yan and Haims (2010), and Khakzad et al. (2014).

3.3 Performance assessment

Considering binary random variables, the developed BN whose parameters are learned from observation data can be used as a binary classifier so as to determine the state of a random variable of interest provided that the states of other variables are known. To assess the performance of the developed BN as a classifier, a number of techniques can be employed among which the method of Receiving Operating Characteristics (ROC) is used in the present study due to its both simplicity and practicality (Cook, 2007).

ROC is widely used in machine learning and data mining (Khakzad et al., 2015); it is created by plotting the classifier's true positive rate (TPR) versus its false positive rate (FPR). TPR is the fraction of true positives out of the total actual positives (a.k.a the sensitivity of the classifier) whereas FPR is the fraction of false positives out of the total actual negatives (a.k.a one minus the specificity of the classifier) at a specific threshold setting:

$$TPR = \frac{TP}{TP+FN} \tag{17}$$

$$FPR = \frac{FP}{FP+TN} \tag{18}$$

where TP is true positives, FP is false positives, FN is false negatives, and TN is true negatives. A ROC space is defined by FPR and TPR as horizontal and vertical coordinate axes, respectively (Figure 6). The line of no discrimination (LND) drawn from the bottom left (0,0) to the top right (1,1) divides the ROC space into three areas: (i) points above the LND illustrate good predictions, (ii) points below the LND represent poor predictions, and (iii) a point along the LND represents random predictions.

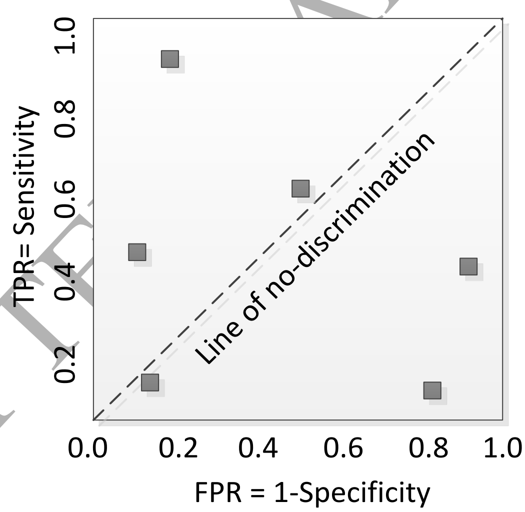

Figure 6. An exemplification of ROC for performance assessment of binary classifiers.

The distance of a point from the LND in either direction indicates the good or poor performance of the respective classifier. The accuracy of the classifier (ACC) can be estimated as:

$$ACC = \frac{TP+TN}{TP+FP+TN+FN} \tag{19}$$

4. An illustrative example

4.1. Case study

To illustrate the application of the developed methodology, a storage tank of crude oil with a diameter of D = 22 m, height of H = 11 m, and shell thickness of t = 0.01 m is considered. The height of crude oil inside the tank is considered to uniformly vary from zero to 0.75 H, that is, h ~ Uniform (0.0 m, 8.25 m). For flood-induced fragility assessment of chemical vessels, a comprehensive flood hazard assessment should be performed to identify the frequency of floods along with relevant parameters such as the height of inundation, S, and flow velocity, V. This demands for an exhaustive investigation of mechanisms that can lead to floods, including extreme precipitation, snow melting, and dam breaks, along with the hydrological and topological aspects of floodplains (Van Gelder, 2013).

In the present study, for illustration purposes only, a hypothetical flood is considered, the height of inundation and the flow velocity of which follow normal distribution as S ~ Normal (μ = 1.0 m, σ = 0.1 m) and V ~ Normal (μ = 2.0 m/s, σ = 0.25 m/s). The parameters and variables used in the present study have been summarized in Table 1.

Table 1. Parameters used for vulnerability assessment of storage tank.

Parameter	Symbol	Value	Unit
Storage tank's height	H	11	m
Storage tank's diameter	D	22	m
Storage tank's shell thickness	t	0.01	m
Crude oil height	h	Uniform (0.0 , 8.25)	m
Flood's inundation height	S	Normal (1.0, 0.1)	m
Flood's flow velocity*	V	Normal (2.0, 0.25)	m/s
Tank shell density (steel)	ρ_s	7900	kg/m^3
Flood water density	ρ_w	1024	kg/m^3
Crude oil density	ρ_l	850	kg/m^3
Young's modulus	E	2.1 E +11	Pa
Buckling critical pressure (Eq. 10)	P_{cr}	217	Pa
Poisson ratio	v	0.3	
Drag coefficient	C_d	1.8	
Friction coefficient	C_f	0.4	
Number of buckling waves	n	2	

4.2. Results

To assess the vulnerability of the storage tank, Monte Carlo simulation is performed (5000 runs) to generate random values of LSEs based on Equations (1), (5), and (11), for flotation, shell buckling, and sliding, respectively. For this purpose, all the parameters are assumed constant except the height of crude oil h, inundation height S, and flow velocity V (Table 1). As such, the positive values of, for example, $LSE_{Flotation}$ indicate the tank flotation (Float = 1), whereas negative values indicate the tank survival (Float = 0). Similarly, the values of $LSE_{Buckling}$ and $LSE_{Sliding}$ can be used to determine the possibilities of shell buckling and sliding.

Taking into account the random variables h, S, and V which contribute to the flotation (Float), shell buckling (Buckle), and rigid sliding (Slide) of the storage tank, the structure of the corresponding BN can be developed as in Figure 7 using GeNIe software[2].

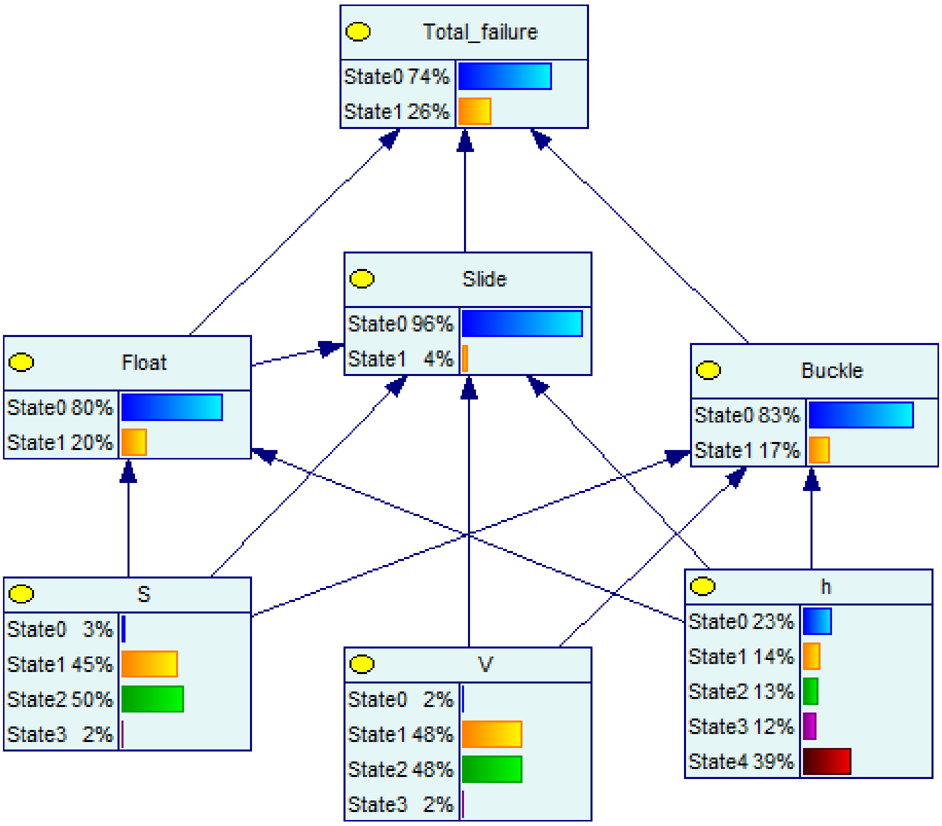

Figure 7. Developed BN for fragility assessment of storage tanks impacted by flood.

As can be seen from Figure 7, the heights of crude oil h and water inundation S contribute to all three failure modes whereas the flow velocity V only plays a role in shell buckling and sliding. Such cause-effect relationships have been denoted by the arcs from h, S, and V to the respective failure modes. Likewise, since the flotation and sliding of the storage tank are mutually exclusive (the former prohibits the latter; see Section 2.3), there is an arc from the node Float to the node Slide to incorporate such conditional dependency, that is, P(Slide= 1 | Float= 1) =0.0.

[2] GeNIe 2.0, Decision Systems Laboratory, University of Pittsburgh, available from: www.bayesfusion.com

It has to be noted that in the nodes Float, Buckle, and Slide, the States 1 and 0 refer to the occurrence and nonoccurrence, respectively, of the failure modes (Table 2). Having the structure of the BN determined, the next step will be to estimate the network parameters (conditional probabilities) based on the generated dataset using the parameter learning algorithm described in Section 3.2. For this purpose, first the generated continuous data for each random variable was discretized into a limited number of states in order to comply with the discrete chance nodes in the BN of Figure 7 as listed in Table 2.

Table 2. States of the variables in the BN of Figure 7.

State	h	S	V	Float	Buckle	Slide
0	0.0 - 1.0	0.0 - 0.8	0.0 - 1.5	LSE < 0	LSE < 0	LSE < 0
1	1.0 - 1.5	0.8 - 1.0	1.5 -2.0	LSE > 0	LSE > 0	LSE > 0
2	1.5 - 2.0	1.0 - 1.2	2.0 -2.5			
3	2.0 - 2.5	> 1.2	> 2.5			
4	> 2.5					

The reason for the discretization of h with more intervals for $0.0 < h < 2.5$ is the fact that the critical height of chemical inside the storage tank, i.e., the height below which the tank becomes floated, has been reported about the flood inundation height, S (RRT6, 2016). Likewise, the discretization of S and V has been carried out owing to the fact that in a normal distribution 95% of the data lies between $\mu \pm 2\sigma$. A sample of data modified according to the foregoing discretization has been depicted in Figure 8.

S	**V**	**h**	**Float**	**Buckle**	**Slide**
2	1	1	0	0	0
1	2	0	1	1	0
1	2	4	0	0	0
2	0	0	1	1	0
1	1	0	1	1	0
2	1	0	0	0	1
2	1	3	0	0	0
1	2	3	0	0	0
1	2	0	1	1	0
2	1	1	0	0	1
2	1	0	1	1	0
2	2	0	1	1	0
1	1	0	1	1	0

Figure 8. Sample data used for BN parameter learning. The numbers refer to the states in Figure 6.

Determinig the parameters of the network, the BN has been run in GeNIe software to calculate the probability of each failure mode along with the probability of the total failure (union of individual failure modes' probabilities via an OR gate), resulting in P(Float) = 0.20, P(Buckle)= 0.17, P(Slide)= 0.04, and P(Total failure) = P(Float ∪ Buckle ∪ Slide) = 0.26 for the flood of interest. Not to mention that ignoring the conditional dependencies[3] among the failure modes would have been resulted in an overestimation of the total failure probability as P(Total failure) = 0.36.

4.3. Verification

The results of the ROC analysis of the developed BN have been displayed in Figure 9 to assess the BN's performance as a classifier. To this end, the dataset generated by Monte Carlo simulation (see Figure 8) in form of {S, V, h, $Float^{MC}$, $Buckle^{MC}$, $Slide^{MC}$} were compared with corresponding data computed by the BN in form of {S, V, h, $Float^{BN}$, $Buckle^{BN}$, $Slide^{BN}$} in order to calculate the parameters needed in Equations (17)-(19).

For sake of clarity, part of calculations carried out for performance assessment of the BN in predicting the flotation have been reported in Table 3 for a number of simulations. In Table 3, in order to make a comparison between the results of Monte Carlo simulation (denoted by MC superscript) with those of the BN analysis (denoted by BN superscript), the flotation probabilities greater than or equal to 0.5 have been taken as State1 (flotation is likely to occur); the numbers in the brackets denote the states.

Table 3. A sample of calculation used for performance assessment of the BN in predicting the flotation. The numbers in the brackets denote the state numbers in Figures 7 and 8.

Simulation ID	S (m)	V (m/s)	H (m)	$Float^{MC}$	$Float^{BN}$	TP	FP	TN	FN
99	1.076 (2)	1.81 (1)	0.78 (0)	LSE > 0 (1)	0.89 (1)	1	0	0	0
279	0.95 (1)	1.86 (1)	0.86 (0)	LSE < 0 (0)	0.79 (1)	0	1	0	0
405	1.04 (2)	2.32 (2)	2.56 (4)	LSE < 0 (0)	0.005 (0)	0	0	1	0

Having the positive and negative predictions for all the dataset determined, Equations (17) and (18) are used to calculate the coordinates of the respective points in Figure 9. As can be seen, ROC curves for all the failure modes lie well above the LND, implying the high performance of the BN in predicting these failure modes. Besides, using Equation (19), the accuracy of the BN in predicting the failure modes are ACC_{Float}= 0.96, ACC_{Buckle} = 0.91, ACC_{Slide} = 0.81, respectively.

A lower accuracy of the model in predicting the sliding failure mode (note part of ROC curve below LND) may be due to issues such as scarcity of positive data (i.e., cases where sliding occurs) rather than ineffectiveness of the BN. This is well evident from Figure 8, where compared to the floating and buckling modes, the sliding mode is less likely to take place (see few-and-far-between 1s in the last column of Figure 8). In this regard, the application of

[3] $P(A \cup B \cup C) = P(A) + P(B) + P(C) - P(A)P(B) - P(A)P(C) - P(B)P(C) + P(A)P(B)P(C)$

larger datasets which may contain more sliding cases in parameter learning may improve the performance of the developed BN in predicting the sliding mode.

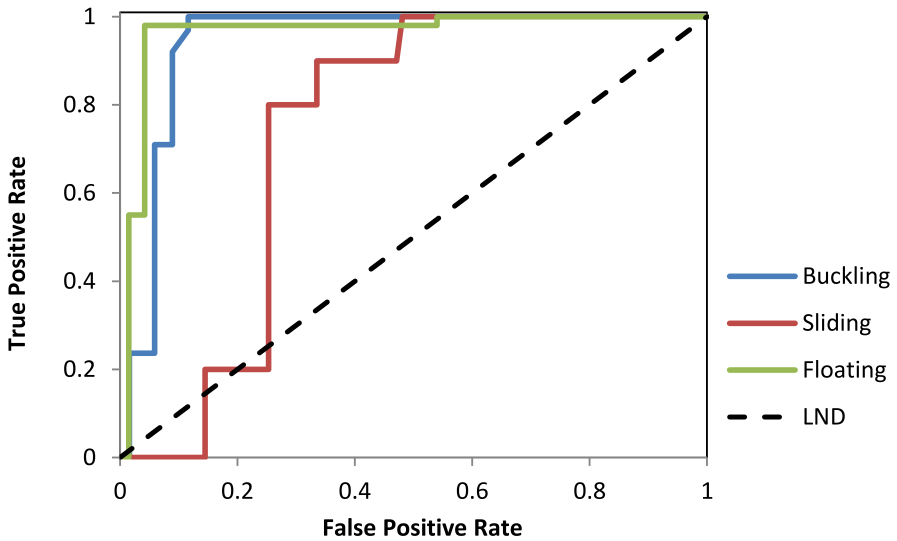

Figure 9. Performance assessment of the BN presented in Figure 6 using ROC technique.

It should be noted that the ROC curves in Figure 9 merely point out the good agreement between the data generated using Monte Carlo simulation based upon physics-of-failure relationships and the data predicted by the developed BN. In other words, Figure 9 should be looked upon as a means of verification of the developed BN (i.e., predicted failure probabilities) assuming that the developed limit state equations (i.e., generated failure probabilities) reasonably resemble (at least with an acceptable level of accuracy) the actual failure mechanisms of equipment in case of floods. That being said, to truly validate the methodology, the generated failure probabilities at the first place should be verified against actual data obtained from either field observations or laboratory experiments. This, however, imposes a challenge since the lack of adequately detailed data is one of the main issues to tackle in flood-related natech risk assessment.

5. Conclusions

In this study we developed a methodology based on Bayesian network to assess the vulnerability of chemical installations to floods. The failure modes such as flotation, buckling, and sliding were modeled in form of limit state equations and coupled with Monte Carlo simulation to generate data required for Bayesian parameter learning. Although the application of the methodology has been demonstrated on petroleum storage tanks, the methodology can readily be tailored to be applicable to a wide variety of process and chemical vessels.

In the present study we illustrated that due attention should be paid to dependencies when combining individual failure modes such as flotation, buckling, and sliding. The dependencies mainly arise due to (i) common load-resistance parameters (e.g., the same flood inundation height, flow velocity, and chemical content) which are taken into account when deriving limit state equations, and (ii) conditional dependencies among the failure modes (e.g., between flotation and sliding). We demonstrated that both types of such dependencies can effectively be taken into account in a Bayesian network methodology, which would otherwise result in an overestimation of the total failure probability.

We illustrated the application of the methodology to flood-related failure of atmospheric storage tanks. Yet, the methodology can be applied, without loss of generality, to a wide variety of natechs (e.g., those triggered by seismic, wind, tsunami, etc.) and industrial plants and infrastructures as long as physical failure mechanisms (in form of limit state equations) can be developed for contributing failure modes.

References

American Society of Civil Engineers (ASCE). Minimum Design Loads for Buildings and Other Structures. ASCE/SEI 7-05. Reston, Virginia. 2006. ISBN: 0-7844-083 1-9.

Antonioni G, Bonvicini S, Spadoni G, Cozzani V. Development of a frame work for the risk assessment of Na-Tech accidental events. Reliability Engineering and System Safety, 2009; 94: 1442–1450.

Antonioni G, Landucci G, Necci A, Gheorghiu D, Cozzani V. Quantitative assessment of risk due to NaTech scenarios caused by floods. Reliability Engineering & System Safety, 2015; 142: 334-345.

API Standard 650. Welded Tanks for Oil Storage. 11th Edition. American Petroleum Institute Publishing Services, Washington. D.C. 2007.

API Standard 620. Design and Construction of Large, Welded, Low-pressure Storage Tanks. 12th Edition. American Petroleum Institute Publishing Services, Washington. D.C. 2013.

Basco A, Salzano E. The vulnerability of industrial equipment to tsunami. Journal of Loss Prevention in the Process Industries (in press): https://doi.org/10.1016/j.jlp.2016.11.009.

Buijs FA, Hall JW, Sayers PB, Van Gelder P. Time-dependent reliability analysis of flood defenses. Reliability Engineering & System Safety, 2009; 94(12): 1942-1953.

Campedel M. Analysis of major industrial accidents triggered by natural events reported in the principal available chemical accident databases. European Commission Joint Research Centre. EUR-Scientific and Technical Research Report: JRC42281. OPOCE. 2008. ISSN: 1018-5593. Available online at http://publications.jrc.ec.europa.eu/repository/handle/JRC42281.

Campedel M, Cozzani V, Garcia-Agreda A, Salzano E. Extending the quantitative assessment of industrial risks to earthquake effects. Risk Analysis, 2008; 28: 1231–1246.

Cook N. Use and misuse of the receiver operating characteristic curve in risk prediction. Circulation, 2007; 115: 928-935.

Cozzani V. Campedel M, Renni E, Krausmann E. Industrial accidents triggered by flood events: analysis of past accidents. Journal of Hazardous Materials, 2010; 175: 501-509.

CNBC (2017). Major refineries are shutting down in the wake of Harvey flooding. 27 Aug 2017. Available at https://www.cnbc.com/2017/08/27/hurricane-harvey-refineries-shutting-down.html.

Cruz AM, Okada N. Consideration of natural hazards in the design and risk management of industrial facilities. Natural Hazards, 2008; 44: 213–227.

Cruz AM, Krausmann E, Franchello G. Analysis of tsunami impact scenarios at an oil refinery. Natural Hazards, 2011; 58: 141–162.

Ebeling C. 2004. An Introduction to Reliability and Maintainability Engineering. Tata McGraw Hill, New Delhi. ISBN-13: 978-0-07-042138-7.

Federal Emergency Management Agency (FEMA). 1995. Engineering principles and practices for retrofitting flood prone residential buildings. FEMA Rep. No. 259, Washington, D.C.

Girgin S, Krausmann E. RAPID_N: Rapid natech risk assessment and mapping framework. Journal of Loss Prevention in the Process Industries, 2013; 26: 949-960.

Godoy LA. Performance of storage tanks in oil facilities damaged by Hurricanes Katrina and Rita. Journal of Performance of Constructed Facilities, 2007; 21(6): 441-449.

Haehnel RB, Daly SF. Maximum impact force of woody debris on floodplain structures. Journal of Hydraulic Engineering, 2004; 130(2): 112-120.

Hauptmanns U. A decision-making framework for protecting process plants from flooding based on fault tree analysis. Reliability Engineering and System Safety, 2010; 95: 970–980.

Hong L, Ouyang M, Peeta S, He X, Yan Y. Vulnerability assessment and mitigation for the Chinese railway system under floods. Reliability Engineering & System Safety, 2015; 137: 58-68.

Iturgaiz Elso M. Finite Element Method studies on the stability behavior of cylindrical shells under axial and radial uniform and non-uniform loads. 2012. Universidad Pública de Navarra, Spain. Available online at http://academica-e.unavarra.es/handle/2454/6186.

Jonkman SN, Lentz A, Vrijling JK. A general approach for the estimation of loss of life due to natural and technological disasters. Reliability Engineering and System Safety, 2010; 95: 1123–1133.

Kameshwar S, Padgett JE. Fragility assessment of above ground petroleum storage tanks under storm surge. 12th International Conference on Applications of Statistics and Probability in Civil Engineering, ICASP 12, Vancouver, Canada, July 12-15, 2015.

Khakzad N, Khakzad S, Khan F. Probabilistic risk assessment of major accidents: application to offshore blowouts in the Gulf of Mexico. Natural Hazards, 2014; 74: 1759–1771.

Khakzad N, Khan F, Amyotte P. Major accidents (Gray Swans) likelihood modeling using accident precursors and approximate reasoning. Risk Analysis, 2015; 35(7): 1336-1347.

Khakzad N, Van Gelder P. Fragility assessment of chemical storage tanks subject to floods. Process Safety and Environmental Protection, 2017; 111: 75-84.

Korkmaz K, Sari A, Carhoglu A. Seismic risk assessment of storage tanks in Turkish industrial facilities. Journal of Loss Prevention in the Process Industries, 2011; 24: 314-320.

Krausmann E, Mushtaq F. A qualitative Natech damage scale for the impact of floods on selected industrial facilities. Natural Hazards, 2008; 46: 179–197.

Krausmann E, Renni E, Campedel M, Cozzani V. Industrial accidents triggered by earthquakes, floods and lightning: lessons learned from a database analysis. Natural Hazards, 2011; 59: 285–300.

Landucci G, Antonioni G, Tugnoli A, Cozzani V. Release of hazardous substances in flood events: damage model for atmospheric storage tanks. Reliability Engineering and System Safety, 2012; 106: 200-216.

Landucci G, Necci A, Antonioni G, Tugnoli A, Cozzani V. Release of hazardous substances in flood events: damage model for horizontal cylindrical vessels. Reliability Engineering and System Safety, 2014; 132: 125-145.

Marzo E, Busini V, Rota R. Definition of a short-cut methodology for assessing the vulnerability of a territory in natural–technological risk estimation. Reliability Engineering and System Safety, 2015; 134: 92–97.

Mebarki A, Jerez S, Prodhomme G, Reimeringer M. Natural hazards, vulnerability and structural resilience: tsunamis and industrial tanks. Geomatics, Natural Hazards and Risk, 2016; 7(S1): 5-17.

Milazzo MF, Ancione G, Basco A, Lister DG, Salzano E, Maschio G. Potential loading damage to industrial storage tanks due to volcanic ash fallout. Natural Hazards, 2013; 66: 939–953.

Neapolitan R. 2003. Learning Bayesian networks. Upper Saddle River, NJ, USA: Prentice Hall, Inc.

Necci A, Antonioni G, Bonvicini S, Cozzani V. Quantitative assessment of risk due to major accidents triggered by lightning. Reliability Engineering and System Safety, 2016; 154: 60–72.

Necci A, Antonioni G, Cozzani V, Krausmann E, Borghetti A, Nucci CA. A model for process equipment damage probability assessment due to lightning. Reliability Engineering and System Safety, 2013; 115: 91–99.

Pearl J. 1988. Probabilistic reasoning in intelligent systems. San Francisco, CA: Morgan Kaufmann.

Rasmussen K. Natural events and accidents with hazardous materials. Journal of Hazardous Materials, 1995; 40: 43–54.

Region 6 Regional Response Team (RRT6). Flood Preparedness. Recommended Best Practices. FactSheet #103, January 2016. Available online at: http://www.deq.louisiana.gov/portal/portals/0/news/pdf/FloodPrepFactSheetDRAFT.pdf.

Renni E, Krausmann E, Cozzani V. Industrial accidents triggered by lightning. Journal of Hazardous Materials, 2010; 184: 42–48.

Salzano E, Garcia Agreda A, Di Carluccio A, Fabbrocino G. Risk assessment and early warning systems for industrial facilities in seismic zones. Reliability Engineering and System Safety, 2009; 94: 1577–1584.

Santella N, Steinberg LJ, Sengul H. Petroleum and hazardous material releases from industrial facilities associated with Hurricane Katrina. Risk Analysis, 2010; 30(4): 635-649.

Sättele M, Bründl M, Straub D. Reliability and effectiveness of early warning systems for natural hazards: Concept and application to debris flow warning. Reliability Engineering and System Safety, 2015; 142: 192–202.

Showalter PS, Myers MF. Natural disasters in the United-States as release agents of oil, chemicals, or radiological materials between 1980 and 1989. Risk Analysis, 1994; 14: 169–181.

Siu NO, Kelly DL. Bayesian parameter estimation in probabilistic risk assessment. Reliability Engineering and System Safety, 1998; 62: 89–116.

Sturgis S. The Katrina oil spill disaster: A harbinger for the Atlantic Coast? Facing South: The online magazine of the Institute for Southern Studies, August 28, 2015. Available online at: https://www.facingsouth.org/2015/08/the-katrina-oil-spill-disaster-a-harbinger-for-the.html.

The guardian (2017). Houston flooding: two explosions take place at Texas chemical plant. Available from https://www.theguardian.com/us-news/2017/aug/31/explosions-flooded-texas-chemical-plant-arkema-crosby.

Van Gelder P. 2013. Flood Risk Management, Quantitative Methods, in Encyclopedia of Environmetrics, El-Shaarawi and Piegorsch (eds), John Wiley & Sons Ltd: Chichester, UK. DOI: 10.1002/9780470057339.

Vrijling JK. Probabilistic design of water defense systems in The Netherlands. Reliability Engineering & System Safety, 2001; 74(3): 337-344.

White F. Fluid Mechanics. 2003. 5th edition. McGraw-Hill, Boston. ISBN-13: 978-0072402179.

Yan Z, Haimes YY. Cross-classified hierarchical Bayesian models for risk-based analysis of complex systems under sparse data. Reliability Engineering and System Safety, 2010; 95: 764–776.

Young S, Balluz L, Malilay J. Natural and technologic hazardous material releases during and after natural disasters: a review. Science of the Total Environment, 2004; 322: 3–20.